Infection and Drug Resistance

Dovepress
Taylor & Francis Group

Open Access Full Text Article

ORIGINAL RESEARCH

Reversible Evolution of Ceftazidime-Avibactam Resistance Driven by bla_{KPC-71} and Aerobactin Loss in ST11-KL64 Hypervirulent *Klebsiella Pneumoniae*

Zhuoyuan Yang[1], Si Xu[2,3], Zhiyou Xiao[2,3], Derong Xu[2,3], Qiaozhen Tao[1]

[1]Department of Psychosomatic Medicine, the First Affiliated Hospital, Jiangxi Medical College, Nanchang University, Nanchang, Jiangxi, 330000, People's Republic of China; [2]Jiangxi Institute of Translational Medicine, the First Affiliated Hospital, Jiangxi Medical College, Nanchang University, Nanchang, Jiangxi, 330000, People's Republic of China; [3]Jiangxi Key Laboratory of Drug Target Discovery and Validation, Jiangxi Medical College, Nanchang University, Jiangxi, 330000, People's Republic of China

Correspondence: Qiaozhen Tao, Email ndyfy05436@ncu.edu.cn

Background: Carbapenem-resistant *Klebsiella pneumoniae* (CRKP) is a major global health threat, and the emergence of ceftazidime-avibactam (CZA)-resistant KPC variants presents an increasing clinical challenge. This study aimed to investigate the in vivo evolution and phenotypic difference of a KPC-2 variant, KPC-71, during CZA therapy.

Methods: Seven CRKP isolates were sequentially collected from a single hospitalized patient over a 147-day period. Whole-genome sequencing, phylogenetic analysis, plasmid profiling, antimicrobial susceptibility testing, and virulence assays (including *Galleria mellonella* infection, siderophore production, and serum resistance) were performed to characterize the evolutionary dynamics and biological consequences of KPC-71.

Results: KPC-71 emerged repeatedly during CZA treatment, replacing KPC-2 and conferring high-level CZA resistance while reducing carbapenem MICs. Withdrawal of CZA resulted in reversion to KPC-2, restoring carbapenem resistance and CZA susceptibility, indicating a reversible resistance trade-off. Phylogenetic analysis revealed clonal expansion of the KPC-71-producing sublineage. Plasmid analysis identified bla_{KPC} genes located on a conserved IncFII/IncR-type plasmid containing an intact ISKpn27-bla_{KPC}-ISKpn6 transposon, while progressive remodeling of an IncFII(pCRY) plasmid in CRKP103 led to chromosomal integration of multiple resistance genes. Notably, the final isolate, CRKP103, exhibited markedly reduced capsule production, siderophore activity, serum survival, and attenuated virulence in *G. mellonella*, which associated with the loss of the *iucABCD*/*iutA* locus on an IncHI1B-type virulence plasmid. Functional validation confirmed that KPC-71 expression alone conferred high-level CZA resistance while modulating susceptibility to other β-lactams.

Conclusion: This study provides the first clinical evidence of the reversible in vivo evolution of an insertional KPC-71 variant under antibiotic pressure. The findings reveal a dynamic balance between resistance and virulence mediated by bla_{KPC} mutations and plasmid remodeling, highlighting the risk of resistance cycling during CZA treatment and the need for genomic surveillance in managing CRKP infections.

Keywords: *Klebsiella pneumoniae*, ST11-KL64, KPC-71, virulence, resistance

Introduction

Klebsiella pneumoniae is an important opportunistic pathogen that colonizes the human gastrointestinal and respiratory tracts, as well as hospital environments.[1,2] It is a leading cause of severe infections such as pneumonia, urinary tract infections, and bloodstream infections.[3] The widespread and often inappropriate use of antibiotics has contributed to the emergence and rapid dissemination of drug-resistant *K. pneumoniae* strains, particularly carbapenem-resistant *K. pneumoniae* (CRKP) carrying *K. pneumoniae* carbapenemase (KPC), which has become a major global public health threat.[4]

Received: 15 September 2025
Accepted: 21 November 2025
Published: 6 December 2025

Among the various mechanisms of carbapenem resistance, KPC-type β-lactamases are the most widely disseminated globally, with KPC-2 and KPC-3 being the predominant variants.[5] Ceftazidime-avibactam (CZA), a novel combination of a third-generation cephalosporin and a non-β-lactam β-lactamase inhibitor, has been introduced into clinical practice and has demonstrated potent activity against most KPC-producing organisms.[6,7] With increasing clinical use of CZA, resistance has frequently arisen through point mutations within the bla_{KPC} gene, particularly in regions affecting the active site or regulatory domains of the enzyme, which alter its affinity for substrates and inhibitors.[8,9] Several CZA-resistant KPC variants have been identified, such as KPC-8, KPC-31, and KPC-33, which evade avibactam inhibition by modifying the conformation of the Ω-loop or catalytic pocket.[10–12] Nevertheless, the in vivo evolution of KPC variants during clinical infection remains poorly characterized, particularly with respect to associated modifications in virulence, representing an important gap in current understanding.

Importantly, increasing virulence among CRKP strains has raised significant concern in recent years.[13] The ST11-KL64 clone, in particular, is frequently associated with hypervirulence genes such as *iucABCD, iutA*, and *rmpA2*, resulting in so-called "superbugs" that combine high levels of resistance and virulence, posing serious challenges to clinical management.[14] However, it remains unclear whether CRKP can modulate virulence under strong antibiotic selection pressure, for example by attenuating pathogenic potential to preserve resistance. The interplay between resistance evolution, virulence dynamics, and plasmid adaptation therefore warrants further investigation.

In this study, we conducted a longitudinal genomic analysis of seven CRKP isolates collected from a single hospitalized patient over a 147-day clinical course. Within-host longitudinal investigations offer a valuable opportunity to directly observe the adaptive evolution of pathogens in real time, capturing the dynamic interplay between antibiotic exposure, resistance development, and virulence modulation that is often overlooked in cross-sectional surveillance. To our knowledge, this is the first clinical observation of the in vivo evolution of a KPC-2 variant, KPC-71. Our findings revealed that the emergence of KPC-71 was closely associated with CZA exposure and was accompanied by distinct changes in antimicrobial susceptibility and virulence. Through whole-genome sequencing, phylogenetic analysis, plasmid profiling, and functional validation, we elucidated the adaptive evolutionary mechanisms of CRKP during antibiotic treatment.

Materials and Methods

Isolate Identification and Culture

A total of seven *K. pneumoniae* isolates were sequentially collected from a single hospitalized patient over a 147-day period at the Department of Clinical Laboratory, First Affiliated Hospital of Nanchang University (Jiangxi, China). Clinical specimens were obtained from sputum and bronchoalveolar lavage fluid (BALF) during routine diagnostic procedures. All samples were processed in accordance with standard microbiological protocols. Initial bacterial isolation was performed using blood agar. Colonies with typical Klebsiella morphology were subcultured for further testing. Species-level identification was conducted using matrix-assisted laser desorption ionization time-of-flight mass spectrometry (MALDI-TOF MS) (Bruker Daltonics, Germany).

Antimicrobial Susceptibility Testing

Antimicrobial susceptibility testing of the seven CRKP isolates was performed using the broth microdilution method with commercially prepared, pre-loaded microdilution panels (Autobio, China), following the manufacturer's instructions. Minimum inhibitory concentrations (MICs) were determined for a wide range of antimicrobial agents, including meropenem, imipenem, fosfomycin, ceftazidime, cefuroxime, cefepime, ceftazidime-avibactam, cefoperazone-sulbactam, piperacillin-tazobactam, amikacin, gentamicin, levofloxacin, moxifloxacin, tigecycline, trimethoprim-sulfamethoxazole, and polymyxin B. Interpretation of MIC results was based on the Clinical and Laboratory Standards Institute (CLSI) guidelines (2024).[15] For tigecycline, interpretive criteria were applied according to the US Food and Drug Administration (FDA) breakpoints, and for polymyxin B, European Committee on Antimicrobial Susceptibility Testing (EUCAST) breakpoints were used. *Escherichia coli* ATCC 25922 and *K. pneumoniae* ATCC 13883 was used as a quality control strain throughout the testing process. Each susceptibility test was performed in triplicate to ensure the reproducibility and reliability of the results.

Whole-Genome Sequencing and Bioinformatics Analysis

Genomic DNA was extracted from each isolate using a commercial DNA extraction kit (Qiagen, Germany) following to the manufacturer's instructions. Whole-genome sequencing (WGS) was performed for all seven CRKP isolates using the Illumina NovaSeq 6000 platform (Illumina, San Diego, CA, USA) with paired-end 150 bp reads. In addition, three representative isolates (CRKP36, CRKP55, and CRKP103) underwent long-read sequencing on the PacBio Sequel platform (Pacific Biosciences, Menlo Park, CA, USA). Genome assemblies were generated using Unicycler v0.5.0,[16] with Illumina short-read assemblies for all isolates and hybrid assemblies for the three representative strains (CRKP36, CRKP55, and CRKP103). Antimicrobial resistance genes, virulence determinants, plasmid replicon types, serotype predictions, and multilocus sequence types (MLST) were identified using the Kleborate v3.1.3, VRprofile2, and PlasmidFinder v2.1 databases,[17–20] applying identity ≥ 90% and coverage ≥ 90% as thresholds. Circular plasmid maps were generated using BRIG (BLAST Ring Image Generator) to visualize genome architecture and plasmid content.[21] To investigate the structural differences between KPC variants, amino acid sequence alignment and secondary structure prediction of KPC-2 and KPC-71 were performed using ESPript 3.0.[22] For phylogenetic analysis, a core genome alignment was constructed using CRKP isolates with *K. pneumoniae* HS11286 (RefSeq: GCF_000240185.1) as the reference genome, using snippy v.4.6.0.[23] Recombination regions were identified and removed with Gubbins v3.2.1.[24] A maximum-likelihood phylogenetic tree was then inferred using FastTree v2.1.11 under the GTR + CAT substitution model,[25] and visualized using the Interactive Tree of Life (iTOL) platform for annotation and presentation.[26]

Capsule Quantification

Uronic acid content was quantified following a previously described protocol.[27] Overnight bacterial cultures were grown in Luria-Bertani (LB) broth at 37 °C with shaking and subsequently diluted 1:100 into fresh LB medium. The cultures were incubated at 37 °C for 6 hours to reach exponential phase. A 500 µL aliquot of each culture was mixed with 100 µL of 1% Zwittergent 3–12 detergent (in 100 mM citric acid buffer, pH 2.0) and incubated at 50 °C for 20 minutes to lyse bacterial cells and release capsular material. The mixture was then centrifuged at 13,000 × g for 5 minutes, and 300 µL of the resulting supernatant was transferred to a new tube and mixed with 1.2 mL of absolute ethanol. After incubation at room temperature for 5 minutes, samples were centrifuged again at 13,000 × g for 5 minutes to pellet the capsular material. The resulting pellet was air-dried and resuspended in 200 µL of sterile distilled water. To quantify uronic acid content, 1.2 mL of sodium tetraborate solution (12.5 mM in concentrated sulfuric acid) was added to each sample, followed by incubation at 100 °C for 5 minutes. Samples were then immediately transferred to ice and cooled for at least 10 minutes. After cooling, 20 µL of m-hydroxydiphenyl reagent was added, and the mixture was incubated at room temperature for 5 minutes. Absorbance was measured at 520 nm using a microplate reader, and uronic acid concentrations were calculated from a standard curve prepared with D-glucuronic acid as the reference compound.

Quantitative Siderophore Production Assay

Quantitative chrome azurol S (CAS) agar assay was performed as previously described.[28] This assay measures the ability of bacteria to chelate iron from a dye–iron complex, resulting in a visible color change. Briefly, bacterial strains were cultured in iron-limited M9 minimal medium until mid-logarithmic phase ($OD_{600} \approx 0.6$). A 1 µL aliquot of the culture was spotted onto freshly prepared CAS agar plates, which contain chrome azurol S dye, $FeCl_3$, and hexadecyltrimethylammonium bromide (HDTMA) to form a blue iron–dye complex. Plates were incubated at 37 °C for 24 hours under aerobic conditions. Following incubation, the formation of a distinct orange halo around the bacterial colony was recorded. The diameter of the orange zone (in millimeters) was measured using a digital caliper and used as a semi-quantitative indicator of siderophore activity. Each assay was performed in triplicate, and the results were reported as mean ± standard deviation.

Serum Resistance Assay

Bacterial cultures were grown in LB broth to mid-logarithmic phase ($OD_{600} \approx 0.6$) and adjusted to a final concentration of 1.5×10^6 CFU/mL in phosphate-buffered saline (PBS). An aliquot of 100 µL bacterial suspension

was mixed with 300 μL of pooled normal human serum (NHS) obtained from healthy adult volunteers who had provided informed consent. The mixture was incubated at 37 °C for 2 hours under gentle shaking to allow interaction between bacteria and complement proteins. Following incubation, samples were serially diluted in PBS and plated onto LB agar to determine the number of viable bacteria by colony counting. Plates were incubated overnight at 37 °C, and CFU counts were recorded. Each assay was performed in biological triplicates.

Galleria Mellonella Infection Model

G. mellonella larvae were obtained from a commercial supplier (Tianjin Huiyude Biotech, Tianjin, China) and stored in the dark at 4 °C prior to use. Only healthy larvae weighing approximately 250–300 mg, with uniform creamy coloration and no signs of melanization, discoloration, or physical damage, were included in the experiments. Bacterial suspensions were grown to mid-log phase, washed twice in PBS, and adjusted to a final concentration of 1×10^6 CFU/mL. Each larva was injected with 10 μL of bacterial suspension through the last left proleg using a fine Hamilton syringe. Control groups were injected with 10 μL of sterile PBS. A minimum of 30 larvae per group were used, divided into three Petri dishes (10 larvae per dish) to account for potential environmental variation. Infected larvae were incubated at 37 °C in the dark, and survival was monitored every 12 hours over a 72-hour period. Larvae were considered dead when they failed to respond to gentle tactile stimulation. Survival data were analyzed using Kaplan-Meier survival curves, and statistical differences between groups were evaluated with the log-rank (Mantel-Cox) test. Two well-characterized reference strains were included: NTUH-K2044, a hypervirulent strain used as a positive control, and ATCC 700603, a classical strain used as a negative control. All experiments were repeated at least three times.

Construction of pDK6-KPC Plasmids

Plasmid constructs carrying different bla_{KPC} variants were generated to evaluate their functional impact. The complete bla_{KPC-2} and bla_{KPC-71} genes, including their native promoter regions, were amplified using PrimeSTAR DNA Polymerase (Takara, Japan; Cat. No. R045A).The complete bla_{KPC-2} and bla_{KPC-71} genes, including their native promoter regions, were amplified with PrimeSTAR DNA Polymerase (Takara, Japan; Cat. No. R045A) using the primers 5′-ACAGGAAACAGAATTCGAGCTCTTGTTCAGGAAACGCGTGTA-3′ and 5′-AGCCAAGCTTGCATGCCTGCAGG GTGGGCCAATAGATGATTTTC-3′. The PCR products were purified and ligated into the pDK6 expression vector using the NEBuilder HiFi DNA Assembly Master Mix (New England Biolabs, USA; Cat. No. E2621), following the manufacturer's instructions. The recombinant plasmids (pDK6-KPC-2 and pDK6-KPC-71) were introduced into chemically competent *E. coli* DH5α cells via heat-shock transformation. Transformants were selected on LB agar plates supplemented with appropriate antibiotics, and positive clones were verified by colony PCR targeting the bla_{KPC} gene followed by Sanger sequencing. Confirmed plasmids were then extracted from *E. coli* DH5α and subsequently introduced into *K. pneumoniae* ATCC 13883 via electroporation using a Gene Pulser Xcell system (Bio-Rad, USA). Transformants were selected and further validated by plasmid profiling and PCR to ensure successful introduction of the KPC variants.

Statistical Analysis

All statistical analyses were performed using GraphPad Prism version 9.0 (GraphPad Software Inc., San Diego, CA, USA). Data were expressed as mean ± standard deviation (SD) from at least three independent biological replicates. Comparisons between multiple groups were conducted using one-way analysis of variance (ANOVA). A p-value < 0.05 was considered statistically significant.

Result

Emergence and Evolution of a KPC-2 Variant (KPC-71) in a Hospitalized Patient

We collected seven CRKP isolates longitudinally from a single 65-year-old male patient who was admitted to the intensive care unit with severe pneumonia and sepsis secondary to chronic obstructive pulmonary disease. The isolates were recovered from respiratory specimens, including sputum and bronchoalveolar lavage fluid, during a 147-day

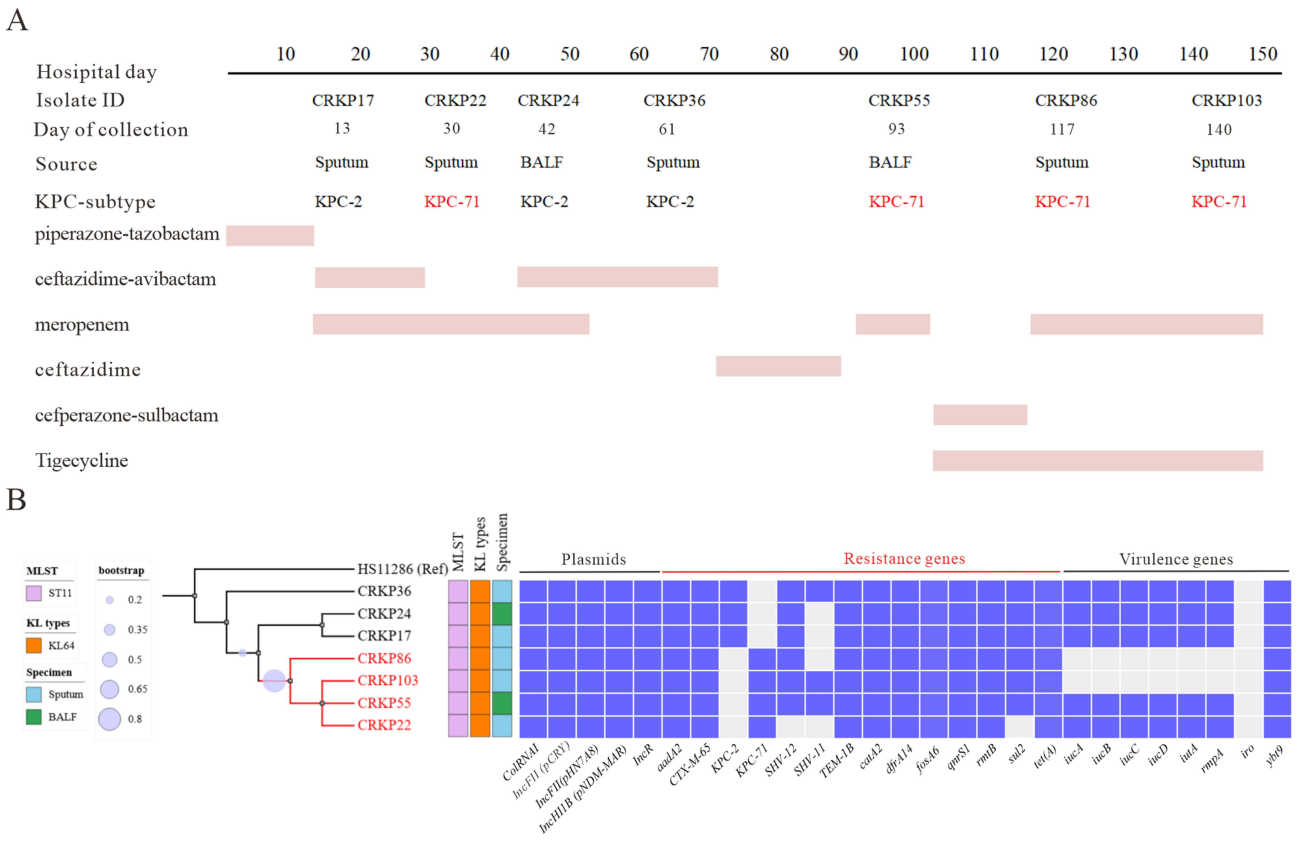

Figure 1 Longitudinal evolution and genomic characterization of CRKP isolates from a hospitalized patient. (**A**) Timeline of seven CRKP isolates collected over a 147-day hospitalization. (**B**) Phylogenetic analysis and genomic features of the seven CRKP isolates. The maximum-likelihood phylogenetic tree was constructed from core genome SNPs, with *K. pneumoniae* HS11286 as the reference.

hospitalization period. The patient initially received empirical piperacillin-tazobactam therapy during the first 12 days of hospitalization for ventilator-associated pneumonia. After the isolation of CRKP, ceftazidime-avibactam (CZA) was introduced on day 13 and continued for 17 days. Meropenem, ceftazidime, cefoperazone-sulbactam, and tigecycline were administered intermittently during the later course of hospitalization in response to recurrent infection episodes (Figure 1A). Each isolate underwent whole-genome sequencing, resistance gene profiling, and antimicrobial susceptibility testing to characterize the molecular trajectory of resistance. The earliest isolate, CRKP17, recovered on day 13 of hospitalization, harbored the $bla_{\text{KPC-2}}$ gene and exhibited high-level resistance to carbapenems (imipenem/meropenem) while remaining susceptible to CZA (Table 1).

Following the initiation of CZA therapy, a genotypic and phenotypic shift was observed. On hospital day 30, CRKP22 was isolated and found to harbor a KPC variant, KPC-71, which conferred resistance to CZA (MIC >16/4 μg/mL) and reduced carbapenem MICs (imipenem and meropenem, MIC = 2 μg/mL). Interestingly, subsequent isolates CRKP24 (day 42) and CRKP36 (day 61) reverted back to KPC-2, accompanied by restoration of CZA susceptibility (MIC = 4/4 μg/mL), but with a return to high-level carbapenem resistance (MICs >16 μg/mL). Later in the treatment course, with the reintroduction of CZA, three additional KPC-71-producing strains, CRKP55 (day 93), CRKP86 (day 117), and CRKP103 (day 140), were recovered. These isolates again exhibited CZA resistance (MIC >16/4 μg/mL) and intermediate susceptibility to imipenem and meropenem (MIC = 2 μg/mL).

All seven isolates displayed multidrug-resistant phenotypes, with resistance to all tested β-lactam/β-lactamase inhibitor combinations (including piperacillin-tazobactam and cefoperazone-sulbactam), extended-spectrum cephalosporins (ceftazidime, cefepime, cefuroxime), aminoglycosides (amikacin and gentamicin), fluoroquinolones (levofloxacin and moxifloxacin), trimethoprim-sulfamethoxazole, polymyxin B, and fosfomycin. Tigecycline remained the sole antimicrobial agent to which all isolates were consistently susceptible (Table 1).

https://doi.org/10.2147/IDR.S565339

Table 1 Antimicrobial Susceptibility Profiles of 7 CRKP Strains in This Study

Antimicrobial agent	CRKP17	CRKP22	CRKP24	CRKP36	CRKP55	CRKP86	CRKP103
	KPC-2	KPC-71	KPC-2	KPC-2	KPC-71	KPC-71	KPC-71
	MIC (μg/mL, S/I/R)						
Meropenem	>16 (R)	2 (I)	>16 (R)	>16 (R)	2 (I)	2 (I)	2 (I)
Imipenem	>16 (R)	2 (I)	>16 (R)	>16 (R)	2 (I)	2 (I)	2 (I)
Fosfomycin	>64 (R)	>64 (R)	>64 (R)	>64 (R)	>64 (R)	>64 (R)	>64 (R)
Ceftazidime	>128 (R)	>128 (R)	>128 (R)	>128 (R)	>128 (R)	>128 (R)	>128 (R)
Cefuroxime	>16 (R)	>16 (R)	>16 (R)	>16 (R)	>16 (R)	>16 (R)	>16 (R)
Cefepime	>32 (R)	>32 (R)	>32 (R)	>32 (R)	>32 (R)	>32 (R)	>32 (R)
Ceftazidime-avibactam	4/4 (S)	>16/4 (R)	4/4 (S)	4/4 (S)	>16/4 (R)	>16/4 (R)	>16/4 (R)
Cefoperazone-sulbactam	64/32 (R)	64/32 (R)	64/32 (R)	64/32 (R)	64/32 (R)	64/32 (R)	64/32 (R)
Piperacillin-tazobactam	32/4 (R)	64/4 (R)	64/4 (R)	32/4 (R)	64/4 (R)	64/4 (R)	32/4 (R)
Amikacin	>64 (R)	>64 (R)	>64 (R)	>64 (R)	>64 (R)	>64 (R)	>64 (R)
Gentamicin	>16 (R)	>16 (R)	>16 (R)	>16 (R)	>16 (R)	>16 (R)	>16 (R)
Levofloxacin	>8 (R)	>8 (R)	>8 (R)	>8 (R)	>8 (R)	>8 (R)	>8 (R)
Moxifloxacin	>2 (R)	>2 (R)	>2 (R)	>2 (R)	>2 (R)	>2 (R)	>2 (R)
Tigecycline	2 (S)	2 (S)	2 (S)	2 (S)	2 (S)	2 (S)	2 (S)
Trimethoprim-sulfamethoxazole	>4/76 (R)	>4/76 (R)	>4/76 (R)	>4/76 (R)	>4/76 (R)	>4/76 (R)	>4/76 (R)
Polymyxin B	32 (R)	32 (R)	32 (R)	32 (R)	32 (R)	32 (R)	32 (R)

Abbreviations: R, resistant; I, intermediate; S, sensitive.

Genomic Characteristics and Phylogenetic Analysis of CRKP Strains

To further explore the genetic relatedness and evolutionary dynamics of the seven CRKP isolates, a phylogenetic analysis based on core genome SNPs was performed (Figure 1B). Genome assembly statistics for these isolates are summarized in Supplementary Table S1. All strains belonged to sequence type ST11 and capsular type KL64. The three KPC-2-producing strains (CRKP17, CRKP24, CRKP36) were genetically closer to the reference strain HS11286. The four KPC-71-producing isolates (CRKP22, CRKP55, CRKP86, CRKP103) formed a separate cluster, suggesting clonal expansion of a KPC-71-producing sublineage. These strains exhibited extremely low SNP differences, ranging from 2 to 4.

Plasmid replicon typing revealed that all isolates harbored multiple plasmid types, including ColRNAI, IncFII (pCRY), IncFII (pHN7A8), and IncHI1B (pNDM-MAR). Resistance gene analysis showed that all isolates carried a broad spectrum of antibiotic resistance genes, including $bla_{\text{CTX-M-65}}$, $bla_{\text{TEM-1B}}$, *catA2, dfrA14, fosA6, qnrS1, rmtB*, and *tet(A)*. All strains harbored either $bla_{\text{KPC-2}}$ or the variant $bla_{\text{KPC-71}}$, while the presence of $bla_{\text{SHV-12}}$ and $bla_{\text{SHV-11}}$ varied among isolates. The amino acid alignment and predicted secondary structure modeling (Figure 2) revealed that KPC-71 differs from the wild-type KPC-2 carbapenemase by an insertion of a serine residue between positions 181 and 182. This structural alteration may influence the binding affinity to β-lactam–β-lactamase inhibitor combinations, potentially contributing to ceftazidime-avibactam resistance. Importantly, most isolates retained key virulence-associated genes commonly linked to hypervirulent *K. pneumoniae*, including the aerobactin siderophore system (*iucABCD* and *iutA*), mucoid phenotype regulator (*rmpA2*), and yersiniabactin biosynthetic cluster (*ybt* genes). In contrast, two isolates, CRKP86 and CRKP103, did not carry *iucABCD* or *iutA*.

Chromosomal and Plasmid-Mediated Antimicrobial Resistance in CRKP36, CRKP55, and CRKP103 Strains

Whole-genome and plasmid profiling of CRKP36, CRKP55, and CRKP103 revealed a conserved chromosomal backbone (~5.46 Mb, GC content ~57.4–57.8%) and five plasmids per strain, collectively encoding a broad spectrum of resistance and virulence genes (Table 2). All three isolates harbored key chromosomal resistance determinants, including $bla_{\text{SHV-11}}$, *sul1, aadA2*, and *fosA6*. Notably, CRKP103 also carried several additional chromosomal resistance genes, including *sul2, catA2, tet(A),* $bla_{\text{LAP-2}}$, and *qnrS1*. Plasmid comparisons revealed the presence of three major replicon types with highly

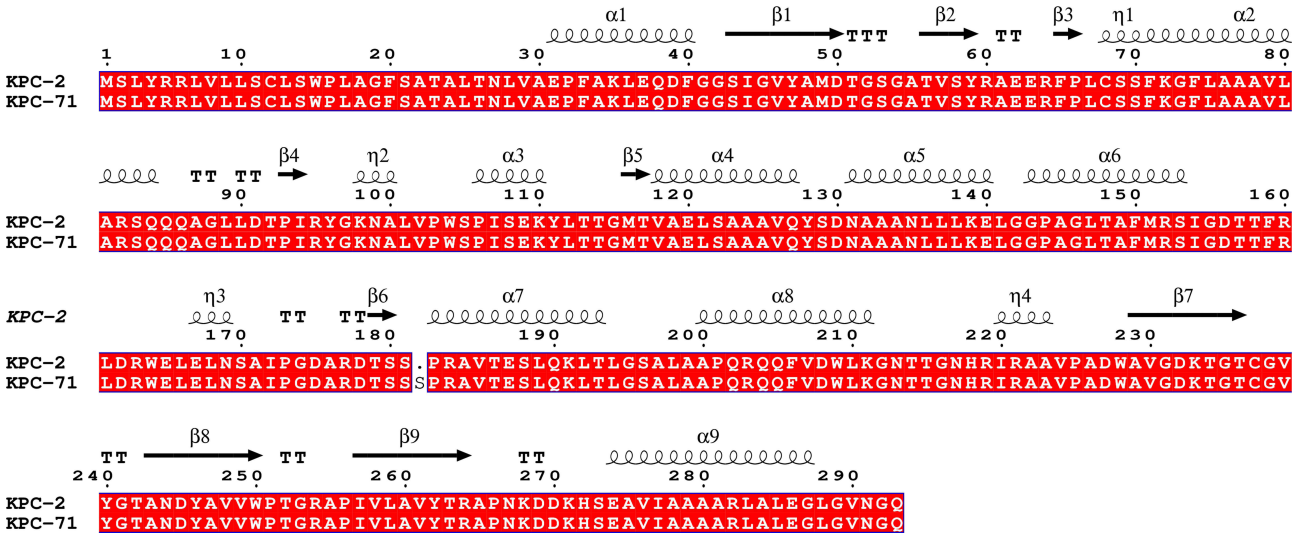

Figure 2 Comparative amino acid sequence alignment and secondary structure prediction of KPC-2 and KPC-71.

conserved backbones across the strains, as visualized in the circular maps (Figure 3). A large IncHI1B-type plasmid (Figure 3A) was detected in all isolates and carried *rmpA2* in all three strains, while encoding the aerobactin siderophore system (*iucABCD*/*iutA*) in CRKP36 and CRKP55 but not in CRKP103. This deletion is clearly visible in the outermost

Table 2 Genomic Characteristics of CRKP36, CRKP55, and CRKP103, Including Chromosomal and Plasmid-Borne Resistance and Virulence Determinants

Strain	Name	Size (bp)	GC Content (%)	Plasmid Type	Resistance Genes	Virulence Factors
CRKP36	Chromosome	5,463,404	57.39	/	*bla*$_{SHV-11}$, *sul1*, *aadA2b*, *fosA6*	/
	pCRKP36-1	195,340	50.32	IncHI1B (pNDM-MAR)	/	*rmpA2*, *iucABCD*/*iutA*
	pCRKP36-2	119,517	53.44	IncFII (pHN7A8)/IncR	*bla*$_{KPC-2}$, *bla*$_{SHV-12}$, *rmtB*, *bla*$_{TEM-1B}$, *bla*$_{CTX-M-65}$	/
	pCRKP36-3	87,095	53.95	IncFII (pCRY)	*dfrA14*, *catA2*, *qnrS1*, *bla*$_{LAP-2}$, *tet(A)*, *sul2*	/
	pCRKP36-4	11,970	55.59	/	/	/
	pCRKP36-5	5,596	51.54	/	/	/
CRKP55	Chromosome	5,464,787	57.81	/	*bla*$_{SHV-11}$, *sul1*, *aadA2b*, *fosA6*	/
	pCRKP55-1	200,047	50.18	IncHI1B (pNDM-MAR)	/	*rmpA2*, *iucABCD*/*iutA*
	pCRKP55-2	119,519	53.44	IncFII (pHN7A8)/IncR	*bla*$_{KPC-71}$, *bla*$_{SHV-12}$, *rmtB*, *bla*$_{TEM-1B}$, *bla*$_{CTX-M-65}$	/
	pCRKP55-3	87,095	53.95	IncFII (pCRY)	*dfrA14*, *catA2*, *qnrS1*, *bla*$_{LAP-2}$, *tet(A)*, *sul2*	/
	pCRKP55-4	11,970	55.59	/	/	/
	pCRKP55-5	5,596	51.54	/	/	/
CRKP103	Chromosome	5,462,944	57.81	/	*bla*$_{SHV-11}$, *sul1*, *aadA2b*, *fosA6*, *sul2*, *catA2*, *tet(A)*, *bla*$_{LAP-2}$, *qnrS1*	/
	pCRKP103-1	169,204	50.19	IncHI1B (pNDM-MAR)	/	*rmpA2*
	pCRKP103-2	119,520	53.44	IncFII (pHN7A8)/IncR	*bla*$_{KPC-71}$, *bla*$_{SHV-12}$, *rmtB*, *bla*$_{TEM-1B}$, *bla*$_{CTX-M-65}$	/
	pCRKP103-3	44,483	53.96	IncFII (pCRY)	*dfrA14*	/
	pCRKP103-4	11,970	55.59	/	/	/
	pCRKP103-5	5,737	51.19	/	/	/

https://doi.org/10.2147/IDR.S565339

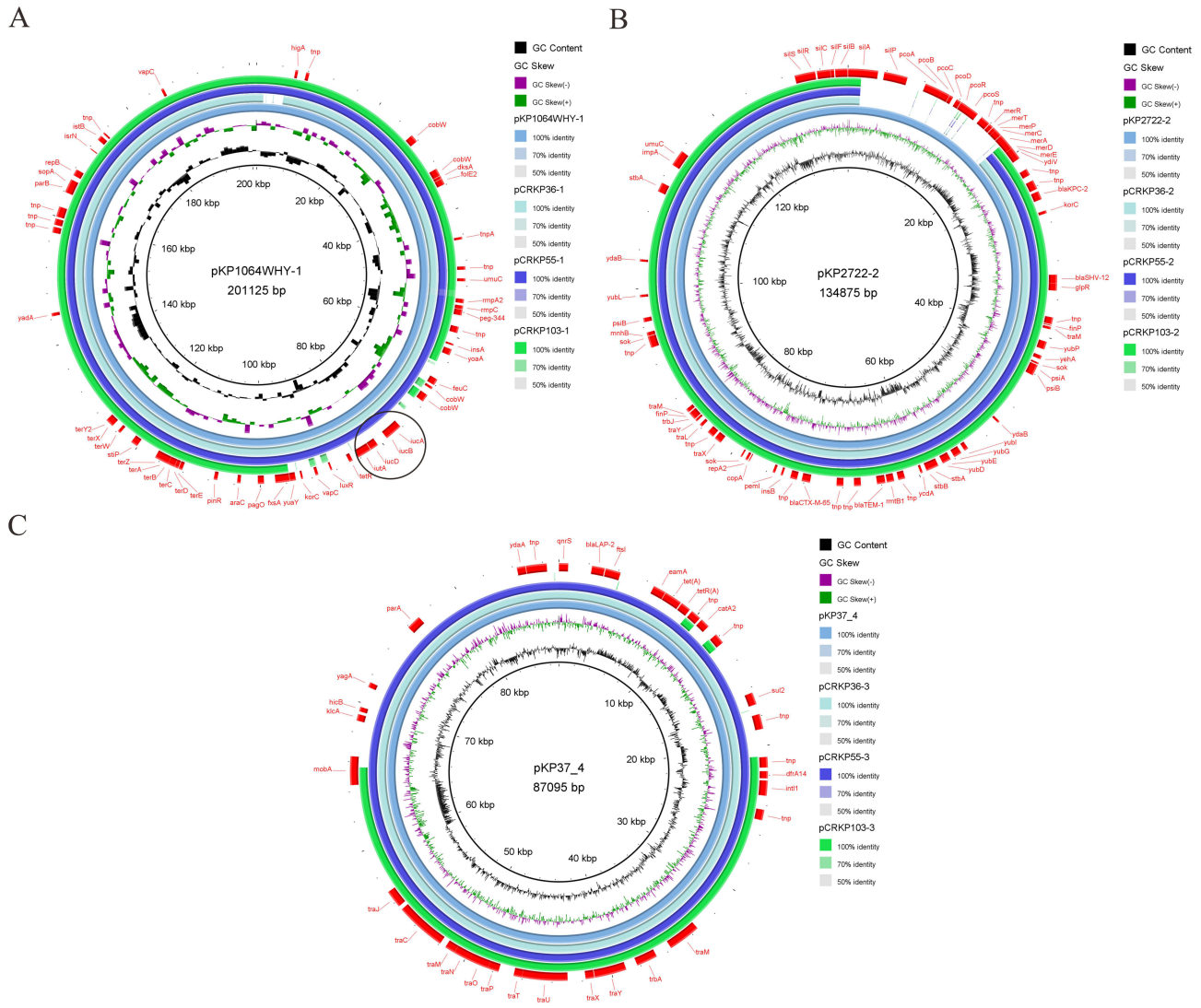

Figure 3 Comparative plasmid maps showing structural conservation and gene content in CRKP36, CRKP55, and CRKP103. (**A**) Alignment of IncHI1B-type plasmids (~201 kb) with reference plasmid pKP1064WHY-1 (CP084706.1). (**B**) Alignment of IncFII(pHN7A8)/IncR plasmids (~135 kb) with reference plasmid pKP2722-2 (CP116905.1). (**C**) Alignment of IncFII(pCRY)-type plasmids (~87 kb in CRKP36/CRKP55, ~44 kb in CRKP103) with reference plasmid pKP37_4 (CP082756.1). Black circles mark the positions corresponding to the *iucABCD/iutA* locus.

rings of the plasmid map, where the *iucABCD* gene cluster is absent in CRKP103-1 but present in CRKP36-1 and CRKP55-1 (Figure 3A).

The IncFII (pHN7A8)/IncR plasmid (Figure 3B) was nearly identical in all strains and carried $bla_{\text{KPC-2}}$ in CRKP36 or $bla_{\text{KPC-71}}$ in CRKP55 and CRKP103. This plasmid also encoded $bla_{\text{SHV-12}}$, $bla_{\text{TEM-1B}}$, $bla_{\text{CTX-M-65}}$, and *rmtB*, conferring resistance to carbapenems, extended-spectrum cephalosporins, and aminoglycosides. The structural conservation of this plasmid is evident in Figure 3B, where all three CRKP strains show high sequence identity with the reference plasmid pKP2722-2 (GenBank accession: CP116905.1). A third multidrug resistance plasmid (~87 kb in CRKP36 and CRKP55, ~44 kb in CRKP103; Figure 3C), identified as IncFII (pCRY)-type, contained *dfrA14, catA2, qnrS1,* $bla_{\text{LAP-2}}$, *tet(A)*, and *sul2* in CRKP36 and CRKP55, while CRKP103 harbored only *dfrA14*. The missing resistance genes (*sul2, catA2, tet(A),* $bla_{\text{LAP-2}}$, and *qnrS1*) were instead found integrated into the chromosome of CRKP103 (Table 2), explaining the reduced coverage observed in the outermost ring of the plasmid map. Additionally, all strains carried two small plasmids (~12 kb and ~5.5 kb) that did not encode any identifiable resistance or virulence determinants. Detailed comparison of the local genetic context surrounding the bla_{KPC} genes revealed a highly conserved *IS26-tnpR-ISKpn27-*bla_{KPC}*-ISKpn6* cassette across all strains (Figure 4).

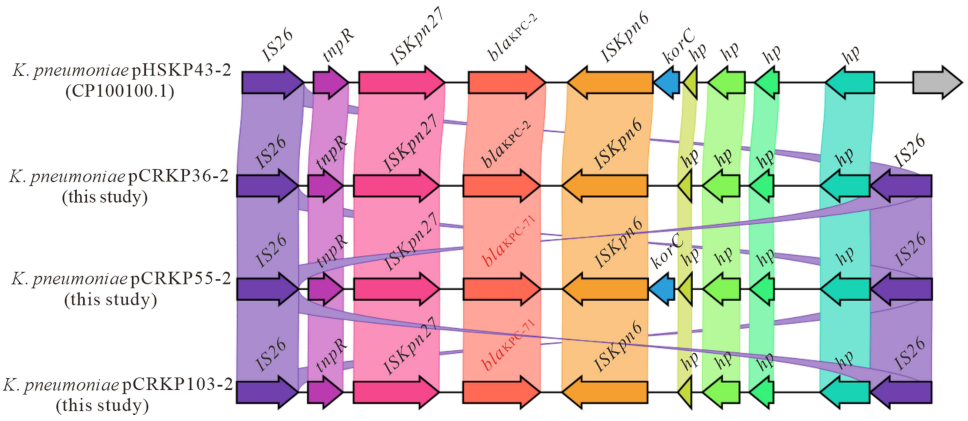

Figure 4 Comparison of the local genetic environment surrounding bla_{KPC-2} (CRKP36) and bla_{KPC-71} (CRKP55 and CRKP103) with the reference plasmid *K. pneumoniae* pHSKP43-2 (GenBank accession: CP100100.1).

CRKP103 Exhibited Lower Virulence Compare CRKP36

Virulence-associated phenotypes were assessed using CPS quantification, siderophore production, serum resistance, cytotoxicity, and in vivo pathogenicity in *G. mellonella* larvae. In the CPS quantification assay (Figure 5A), both CRKP36 and CRKP55 produced significantly higher uronic acid levels (374.33 ± 11.34 mg/L and 370.17 ± 20.61 mg/L, respectively) than the low-virulence control ATCC700603 (130.83 ± 13.24 mg/L), while remaining slightly below the hypervirulent reference NTUH-K2044 (431.17 ± 14.59 mg/L). In contrast, CRKP103 exhibited markedly reduced capsule

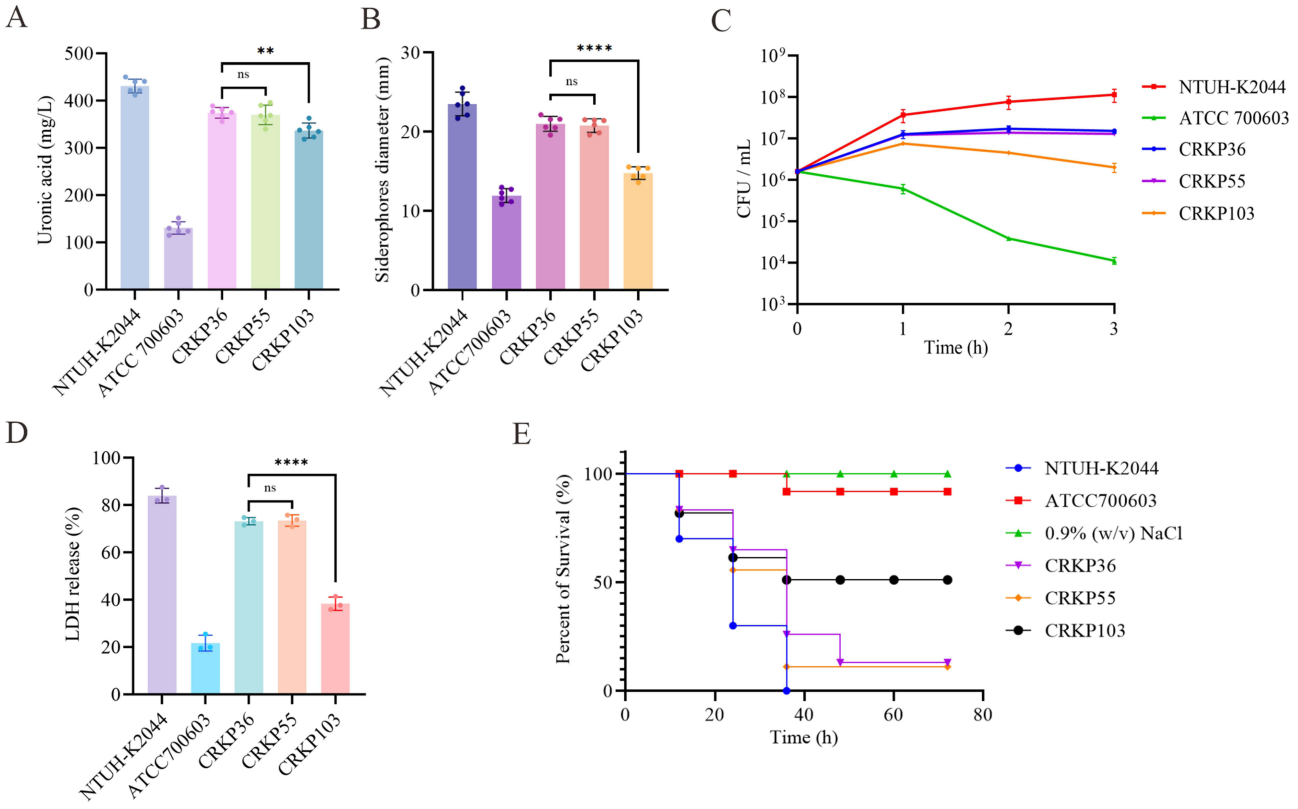

Figure 5 Phenotypic comparison of three CRKP isolates with different resistance and virulence profiles. (**A**) Capsule production measured by uronic acid quantification. (**B**) Siderophore production assessed by chrome azurol S assay. (**C**) Serum resistance. (**D**) Cytotoxicity evaluated by LDH release from A549 epithelial cells after 6 hours of infection. (**E**) In vivo virulence evaluated using the *G. mellonella* infection model. NTUH-K2044 and ATCC 700603 were used as hypervirulent and low-virulence controls, respectively. Data are presented as mean ± standard deviation. $P < 0.01$ (**), $P < 0.0001$ (**), and "ns" indicates no significant difference.

https://doi.org/10.2147/IDR.S565339

production (336.87 ± 16.04 mg/L). In the siderophore production assay (Figure 5B), CRKP103 displayed a smaller halo diameter (14.78 ± 0.79 mm) relative to CRKP36 (20.97 ± 0.94 mm) and CRKP55 (20.78 ± 0.86 mm), both of which were comparable to NTUH-K2044. In the serum resistance assay (Figure 5C), CRKP103 demonstrated a reduced survival rate in 50% human serum, with bacterial counts declining over time. In contrast, CRKP36 and CRKP55 maintained stable bacterial loads comparable to NTUH-K2044, indicating robust serum resistance. The LDH release assay (Figure 5D) revealed that CRKP103 induced significantly lower cytotoxicity toward A549 epithelial cells (38.28 ± 2.81%) compared with CRKP36 (73.14 ± 1.56%) and CRKP55 (73.48 ± 2.43%), which again did not differ significantly from NTUH-K2044 (83.95 ± 3.08%). In the *G. mellonella* infection model (Figure 5E), larvae infected with CRKP103 exhibited significantly higher survival rates (50% at 72 h) than those infected with CRKP36 or CRKP55 (each 10%), further confirming the attenuated in vivo virulence of CRKP103. No significant difference in larval mortality was observed between CRKP36 and CRKP55. Collectively, these results demonstrate that CRKP103 exhibited consistent attenuation of virulence across all assays, in line with the loss of key virulence loci.

K. Pneumoniae Carrying bla_{KPC-71} Exhibited High-Level Resistance to CZA

Compared to the wild-type KPC-2 carbapenemase, KPC-71 contains a disruptive in-frame insertion of three nucleotides (c.540_542dupATC), resulting in the duplication of a serine residue at position 181 (p. Ser181dup). This insertion lies immediately adjacent to the canonical Ω-loop (residues 164–179), a structural motif essential for substrate recognition and inhibitor binding. To assess the phenotypic impact of KPC-71, we cloned bla_{KPC-71} into the pDK6 vector and transformed it into *K. pneumoniae* ATCC 13883. Isogenic strains carrying bla_{KPC-2} or the empty vector were constructed in parallel (Table 3). Antimicrobial susceptibility testing revealed that KPC-71-producing strains exhibited high-level CZA resistance (MIC >16/4 μg/mL), in contrast to the KPC-2-producing counterpart (MIC = 4/4 μg/mL). Similarly, ceftazidime MICs increased from 4 μg/mL (KPC-2) to 64 μg/mL (KPC-71). Interestingly, KPC-71 expression led to a significant reduction in carbapenem MICs, with both imipenem and meropenem MICs decreasing to 2 μg/mL, compared to ≥16 μg/mL in the KPC-2 background. Furthermore, KPC-71 restored susceptibility to several β-lactam/β-lactamase inhibitor combinations previously ineffective in the KPC-2 background, including piperacillin-tazobactam and cefoperazone-sulbactam.

Table 3 Antimicrobial Susceptibility Profiles of *K. Pneumoniae* ATCC 13883 Strains Expressing KPC-2, KPC-71, or Empty Vector

Antimicrobial agent	pDK6-bla_{KPC-2}	pDK6-bla_{KPC-71}	pDK6 (empty vector)
Meropenem	>16 (R)	2 (I)	0.12 (S)
Imipenem	16 (R)	2 (I)	1 (S)
Fosfomycin	≤4 (S)	≤4 (S)	≤4 (S)
Ceftazidime	4 (S)	64 (R)	0.25 (S)
Cefuroxime	>16 (R)	4 (S)	4 (S)
Cefepime	2 (S)	0.5 (S)	0.5 (S)
Ceftazidime-avibactam	4/4 (S)	>16/4 (R)	4/4 (S)
Cefoperazone-sulbactam	64/8 (R)	16/8 (S)	16/8 (S)
Piperacillin-tazobactam	>128/4 (R)	4/4 (S)	4/4 (S)
Amikacin	≤16 (S)	≤16 (S)	≤16 (S)
Gentamicin	≤2 (S)	≤2 (S)	≤2 (S)
Levofloxacin	0.25 (S)	0.25 (S)	0.25 (S)
Moxifloxacin	0.25 (S)	0.25 (S)	0.25 (S)
Tigecycline	≤0.5 (S)	≤0.5 (S)	≤0.5 (S)
Trimethoprim/sulfamethoxazole	≤0.5/9.5 (S)	≤0.5/9.5 (S)	≤0.5/9.5 (S)
Polymyxin B	0.25 (S)	0.25 (S)	0.25 (S)

Discussion

The evolutionary dynamics of CRKP remain a major challenge in antimicrobial resistance research.[29,30] Previous studies have reported that point mutations in bla_{KPC} can mediate CZA resistance, including the emergence of KPC-71.[31] Our study expands this knowledge by providing the first longitudinal clinical evidence that the insertional variant KPC-71 can arise through a stepwise and reversible evolutionary process in vivo. By analyzing seven ST11-KL64 CRKP isolates collected over 147 days, we traced the adaptive trajectory from KPC-2 to KPC-71 and back, revealing how selective antibiotic exposure drives alternating phenotypic and genotypic states.

The emergence of KPC-71 coincided with CZA therapy and was associated with high-level resistance to CZA but reduced carbapenem MICs (Table 1). Previous work demonstrated that the Ser181 duplication in KPC-71 diminishes hydrolytic activity while increasing substrate affinity for ceftazidime, thereby compromising the inhibitory effect of avibactam and potentially explaining the resistance phenotype observed in our isolates.[31] Conversely, following CZA withdrawal, several isolates reverted to KPC-2, restoring carbapenem resistance and resensitization to CZA. This evolutionary pattern suggests repeated selection and re-emergence of the bla_{KPC-71} variant in response to CZA exposure, and its reversion to bla_{KPC-2} in the absence of pressure. This cyclical pattern underscores the capacity of CRKP to exploit a resistance trade-off, dynamically balancing susceptibility to carbapenems and β-lactam/β-lactamase inhibitor combinations.[32] Similar trade-offs have been described for Ω-loop variants such as KPC-31 and KPC-50, which confer resistance to CZA but reduce carbapenem hydrolysis.[11,33] However, unlike these irreversible point mutations, our longitudinal analysis highlights that insertional variants such as KPC-71 can both emerge and regress in vivo, reflecting a more flexible evolutionary strategy.[34,35] These findings suggest that selective pressure from CZA monotherapy may inadvertently promote recurrent selection of resistant variants, highlighting the potential clinical risk of treatment failure and resistance cycling.

Both KPC-2 and KPC-71 were carried on highly conserved IncFII(pHN7A8)/IncR plasmids, embedded within a stable *IS26-tnpR-ISKpn27-*bla_{KPC}*-ISKpn6* transposon, suggesting that the emergence of KPC-71 is driven by local mutational events rather than horizontal acquisition. However, adaptive plasmid remodeling was particularly evident in the final isolate CRKP103. This strain exhibited loss of the *iucABCD*/*iutA* aerobactin cluster from its IncHI1B plasmid, accompanied by reduced siderophore production, impaired serum resistance, diminished capsular polysaccharide synthesis, and attenuated virulence in the *G. mellonella* model, suggesting a potential reduction in hypervirulence potential despite maintaining extensive antimicrobial resistance. While the loss of the *iucABCD*/*iutA* cluster likely contributes to the observed virulence attenuation, other factors such as plasmid burden and associated metabolic costs may also play a role in shaping these phenotypic changes. These changes suggest that resistance evolution may be coupled with virulence attenuation, allowing CRKP to optimize survival while reducing fitness costs in the host environment.

Furthermore, truncation of the IncFII(pCRY) plasmid in CRKP103 (from ~87 kb to ~44 kb) was associated with the loss of accessory resistance genes (*catA2, qnrS1,* bla_{LAP-2}*, tet(A), sul2*). Interestingly, several of these genes were subsequently integrated into the chromosome (Table 2), reflecting a genomic reorganization strategy that may stabilize essential resistance determinants while reducing plasmid burden. The absence of *iucABCD*/iutA and partial loss of resistance elements in CRKP103 suggest progressive plasmid remodeling and potential virulence attenuation during host adaptation or antimicrobial pressure. The role of plasmid remodeling observed in CRKP103 also aligns with reports that resistance gene loss or chromosomal integration can stabilize bacterial fitness in the absence of strong selective pressure.[36,37] Zongo et al recently demonstrated that chromosomal integration of plasmid-borne resistance genes can be actively promoted by an antiplasmid system (ApsAB), which destabilizes costly plasmids while preserving ARGs in carbapenemase-producing *E. coli*.[36] Similarly, Abe et al showed that chromosomally integrated carbapenemase genes can act as long-term reservoirs and may be released back onto plasmids under carbapenem pressure, amplifying resistance and dissemination.[38,39] Our data are consistent with these observations, as multiple resistance genes originally plasmid-borne in CRKP36/55 were integrated into the chromosome of CRKP103. Together, this suggests that CRKP employs both plasmid remodeling and chromosomal assimilation to balance resistance stability, fitness costs, and transmissibility.

From a clinical perspective, these findings carry important implications. The "evolutionary pendulum" we observed underscores the risk that CZA monotherapy may foster cycles of resistance gain and loss, ultimately complicating

treatment outcomes and promoting persistence of resistant subclones.[40] This echoes recent reports where CZA-resistant but carbapenem-susceptible isolates emerged during therapy, only to revert under carbapenem pressure.[41] The decoupling of resistance and virulence traits, as demonstrated by CRKP55 and CRKP103, indicates that low-virulence but highly resistant clones may persist as hidden reservoirs in immunocompromised patients, facilitating silent dissemination of resistance determinants within healthcare settings.

Despite the detailed genomic and phenotypic analyses, several limitations should be acknowledged. First, this work was based on isolates from a single patient, and the limited sample size restricts the ability to generalize our findings to broader epidemiological settings. Second, although plasmid remodeling coincided with virulence attenuation, causality cannot be firmly established without validation in larger cohorts and vertebrate animal infection models, since the *G. mellonella* model has inherent limitations in recapitulating the pathogenicity of *K. pneumoniae* in humans. Finally, the impact of different therapeutic regimens on the observed evolutionary trajectory was not assessed and warrants further investigation.

In conclusion, this study provides the first clinical evidence for the reversible in vivo evolution of the insertional KPC-71 variant in CRKP under antibiotic pressure. We demonstrate how bla_{KPC} mutations and plasmid remodeling jointly shape a dynamic balance between resistance and virulence. The integration of genomic surveillance into clinical practice could inform antimicrobial stewardship and support precision-guided therapeutic decision-making to curb the emergence of resistant subclones. These findings extend current knowledge of adaptive evolution in multidrug-resistant pathogens and underscore the need for longitudinal resistance monitoring and precision-based therapeutic strategies, particularly during CZA treatment.

Data Sharing Statement

The genome sequences in this study have been submitted to NCBI GenBank under accession number PRJNA1314856.

Ethics Statement

This study was reviewed and approved by the Ethics Committee of the First Affiliated Hospital of Nanchang University, Jiangxi, China (Approval Number: (2024)CDYFYYLK(09-010)). The study was conducted in accordance with the ethical principles outlined in the Declaration of Helsinki. Written informed consent was obtained from the patient for the use of clinical isolates and serum samples for research purposes. Experiments involving *Galleria mellonella* larvae were performed in compliance with the institutional guidelines for the care and use of invertebrate animals, which are exempt from formal ethical approval.

Author Contributions

All authors made a significant contribution to the work reported, whether that is in the conception, study design, execution, acquisition of data, analysis and interpretation, or in all these areas; took part in drafting, revising or critically reviewing the article; gave final approval of the version to be published; have agreed on the journal to which the article has been submitted; and agree to be accountable for all aspects of the work.

Funding

The authors received no financial support for the research, authorship, and/or publication of this article.

Disclosure

The authors declare that they have no competing interests.

References

1. Abbas R, Chakkour M, Zein El Dine H, et al. General overview of *Klebsiella pneumonia*: epidemiology and the role of siderophores in its pathogenicity. *Biology*. 2024;13(2):78. doi:10.3390/biology13020078

2. Hussein RA, Al-Kubaisy SH, Al-Ouqaili MTS. The influence of efflux pump, outer membrane permeability and β-lactamase production on the resistance profile of multi, extensively and pandrug resistant *Klebsiella pneumoniae*. *J Infect Public Health*. 2024;17(11):102544. doi:10.1016/j.jiph.2024.102544
3. Paczosa MK, Mecsas J. *Klebsiella pneumoniae*: going on the offense with a strong defense. *Microbiol Mol Biol Rev MMBR*. 2016;80(3):629–661. doi:10.1128/MMBR.00078-15
4. Jiang J, Wang L, Hu Y, et al. Global emergence of carbapenem-resistant hypervirulent *Klebsiella pneumoniae* driven by an IncFIIK34 KPC-2 plasmid. *eBioMedicine*. 2025;113:105627. doi:10.1016/j.ebiom.2025.105627
5. Lee C-R, Lee JH, Park KS, et al. Global dissemination of carbapenemase-producing *Klebsiella pneumoniae*: epidemiology, genetic context, treatment options, and detection methods. *Front Microbiol*. 2016;7:895. doi:10.3389/fmicb.2016.00895
6. Sharma R, Park TE, Moy S. Ceftazidime-Avibactam: a Novel Cephalosporin/β-Lactamase Inhibitor Combination for the Treatment of Resistant Gram-negative Organisms. *Clin Ther*. 2016;38(3):431–444. doi:10.1016/j.clinthera.2016.01.018
7. Al-Ouqaili DMTS. Molecular detection of medically important carbapenemases genes expressed by metallo-î2-lactamase producer isolates of pseudomonas aeruginosa and *Klebsiella pneumoniae*. *Asian J Pharm AJP*. 2018;12(03).
8. Gaibani P, Giani T, Bovo F, et al. Resistance to Ceftazidime/Avibactam, Meropenem/Vaborbactam and Imipenem/Relebactam in Gram-Negative MDR Bacilli: molecular Mechanisms and Susceptibility Testing. *Antibiotics*. 2022;11(5):628. doi:10.3390/antibiotics11050628
9. Al-Ouqaili MTS, Hussein RA, Kanaan BA, et al. Investigation of carbapenemase-encoding genes in Burkholderia cepacia and Aeromonas sobria isolates from nosocomial infections in Iraqi patients. *PLoS One*. 2025;20(8):e0315490. doi:10.1371/journal.pone.0315490
10. Mateo-Vargas MA, Rodríguez-Pallares S, Arca-Suárez J, et al. Emergence of KPC-8-producing *K. pneumoniae* infection without prior exposure to ceftazidime/avibactam: the threat of de novo infections by ceftazidime/avibactam-resistant KPC variants. *Antimicrob Agents Chemother*. 2025;69(6):e01494–24. doi:10.1128/aac.01494-24
11. Faccone D, de Mendieta JM, Albornoz E, et al. Emergence of KPC-31, a KPC-3 variant associated with ceftazidime-avibactam resistance, in an extensively drug-resistant ST235 pseudomonas aeruginosa clinical isolate. *Antimicrob Agents Chemother*. 2022;66(11):e00648–22. doi:10.1128/aac.00648-22
12. Jiang M, Sun B, Huang Y, et al. Diversity of ceftazidime-avibactam resistance mechanism in KPC2-producing *klebsiella pneumoniae* under antibiotic selection pressure. *Infect Drug Resist*. 2022;15:4627–4636. doi:10.2147/IDR.S371285
13. Wu C, Huang Y, Zhou P, et al. Emergence of hypervirulent and carbapenem-resistant *Klebsiella pneumoniae* from 2014 - 2021 in Central and Eastern China: a molecular, biological, and epidemiological study. *BMC Microbiol*. 2024;24(1):465. doi:10.1186/s12866-024-03614-9
14. Chen T, Ying L, Xiong L. Understanding carbapenem-resistant hypervirulent *Klebsiella pneumoniae*: key virulence factors and evolutionary convergence. *hLife*. 2024;2(12):611–624. doi:10.1016/j.hlife.2024.06.005
15. *Performance Standards for Antimicrobial Susceptibility Testing*. 34th. CLSI document M100. Clinical and Laboratory Standards Institute;2024.
16. Wick RR, Judd LM, Gorrie CL, et al. Unicycler: resolving bacterial genome assemblies from short and long sequencing reads. *PLoS Comput Biol*. 2017;13(6):e1005595. doi:10.1371/journal.pcbi.1005595
17. Lam MMC, Wick RR, Watts SC, et al. A genomic surveillance framework and genotyping tool for *Klebsiella pneumoniae* and its related species complex. *Nat Commun*. 2021;12(1):4188. doi:10.1038/s41467-021-24448-3
18. Wyres KL, Wick RR, Gorrie C, et al. Identification of Klebsiella capsule synthesis loci from whole genome data. *Microb Genomics*. 2016;2(12):e000102. doi:10.1099/mgen.0.000102
19. Wang M, Goh Y-X, Tai C, et al. VRprofile2: detection of antibiotic resistance-associated mobilome in bacterial pathogens. *Nucleic Acids Res*. 2022;50(W1):W768–W773. doi:10.1093/nar/gkac321
20. Carattoli A, Zankari E, García-Fernández A, et al. In silico detection and typing of plasmids using PlasmidFinder and plasmid multilocus sequence typing. *Antimicrob Agents Chemother*. 2014;58(7):3895–3903. doi:10.1128/AAC.02412-14
21. Alikhan N-F, Petty NK, Ben Zakour NL, et al. BLAST ring image generator (BRIG): simple prokaryote genome comparisons. *BMC Genomics*. 2011;12(1):402. doi:10.1186/1471-2164-12-402
22. Robert X, Gouet P. Deciphering key features in protein structures with the new ENDscript server. *Nucleic Acids Res*. 2014;42(Web Server issue):W320–324. doi:10.1093/nar/gku316
23. Connor CH, Higgs CK, Horan K, et al. Rapid, reference-free identification of bacterial pathogen transmission using optimized split k-mer analysis. *Microb Genomics*. 2025;11(3):001347. doi:10.1099/mgen.0.001347
24. Croucher NJ, Page AJ, Connor TR, et al. Rapid phylogenetic analysis of large samples of recombinant bacterial whole genome sequences using Gubbins. *Nucleic Acids Res*. 2015;43(3):e15. doi:10.1093/nar/gku1196
25. Price MN, Dehal PS, Arkin AP. FastTree: computing large minimum evolution trees with profiles instead of a distance matrix. *Mol Biol Evol*. 2009;26(7):1641–1650. doi:10.1093/molbev/msp077
26. Letunic I, Bork P. Interactive tree of life (iTOL) v6: recent updates to the phylogenetic tree display and annotation tool. *Nucleic Acids Res*. 2024;52(W1):W78–W82. doi:10.1093/nar/gkae268
27. Wang W, Tian D, Hu D, et al. Different regulatory mechanisms of the capsule in hypervirulent *Klebsiella pneumonia*: "direct" wcaJ variation vs. "indirect" rmpA regulation. *Front Cell Infect Microbiol*. 2023;13:1108818. doi:10.3389/fcimb.2023.1108818
28. Tian D, Wang W, Li M, et al. Acquisition of the conjugative virulence plasmid from a CG23 hypervirulent *Klebsiella pneumoniae* strain enhances bacterial virulence. *Front Cell Infect Microbiol*. 2021;11:752011. doi:10.3389/fcimb.2021.752011
29. Navon-Venezia S, Kondratyeva K, Carattoli A. *Klebsiella pneumoniae*: a major worldwide source and shuttle for antibiotic resistance. *FEMS Microbiol Rev*. 2017;41(3):252–275. doi:10.1093/femsre/fux013
30. Al-Ouqaili DMTS. Molecular detection and sequencing of SHV gene encoding for extended-spectrum Î2-lactamases produced by multidrug resistance some of the gram-negative bacteria. *Int J Green Pharm IJGP*. 2018;12(04).
31. Li X, Ke H, Wu W, et al. Molecular mechanisms driving the in vivo development of KPC-71-mediated resistance to ceftazidime-avibactam during treatment of carbapenem-resistant *Klebsiella pneumoniae* infections. *mSphere*. 2021;6(6):e00859–21. doi:10.1128/mSphere.00859-21
32. Russ D, Glaser F, Shaer Tamar E, et al. Escape mutations circumvent a tradeoff between resistance to a beta-lactam and resistance to a beta-lactamase inhibitor. *Nat Commun*. 2020;11(1):2029. doi:10.1038/s41467-020-15666-2
33. Poirel L, Vuillemin X, Juhas M, et al. KPC-50 confers resistance to ceftazidime-avibactam associated with reduced carbapenemase activity. *Antimicrob Agents Chemother*. 2020;64(8):e00321–20. doi:10.1128/AAC.00321-20

34. Pal A, Andersson DI. Bacteria can compensate the fitness costs of amplified resistance genes via a bypass mechanism. *Nat Commun*. 2024;15(1):2333. doi:10.1038/s41467-024-46571-7
35. Jordana-Lluch E, Barceló IM, Escobar-Salom M, et al. The balance between antibiotic resistance and fitness/virulence in Pseudomonas aeruginosa: an update on basic knowledge and fundamental research. *Front Microbiol*. 2023;14:1270999.
36. Zongo PD, Cabanel N, Royer G, et al. An antiplasmid system drives antibiotic resistance gene integration in carbapenemase-producing Escherichia coli lineages. *Nat Commun*. 2024;15(1):4093. doi:10.1038/s41467-024-48219-y
37. Rajer F, Sandegren L. The role of antibiotic resistance genes in the fitness cost of multiresistance plasmids. *mBio*. 2022;13(1):e03552–21. doi:10.1128/mbio.03552-21
38. Abe R, Akeda Y, Sugawara Y, et al. Carbapenem triggers dissemination of chromosomally integrated carbapenemase genes via conjugative plasmids in Escherichia coli. *mSystems*. 2023;8(3):e0127522. doi:10.1128/msystems.01275-22
39. Owaid HA, Al-Ouqaili MTS. Molecular characterization and genome sequencing of selected highly resistant clinical isolates of Pseudomonas aeruginosa and its association with the clustered regularly interspaced palindromic repeat/Cas system. *Heliyon*. 2025;11(1):e41670. doi:10.1016/j.heliyon.2025.e41670
40. Onorato L, Di Caprio G, Signoriello S, et al. Efficacy of ceftazidime/avibactam in monotherapy or combination therapy against carbapenem-resistant Gram-negative bacteria: a meta-analysis. *Int J Antimicrob Agents*. 2019;54(6):735–740. doi:10.1016/j.ijantimicag.2019.08.025
41. Zhou P, Gao H, Li M, et al. Characterization of a novel KPC-2 variant, KPC-228, conferring resistance to ceftazidime-avibactam in an ST11-KL64 hypervirulent *Klebsiella pneumoniae*. *Int J Antimicrob Agents*. 2025;65(3):107411. doi:10.1016/j.ijantimicag.2024.107411